Mechanism of Corrosion of Cast Aluminum-Silicon Alloys in Seawater. Part 2: Characterization and Field Testing of Sol-Gel-Coated Alloys in the Adriatic Sea

Ingrid Milošev,[‡,] Peter Rodič,[*] Barbara Kapun,[*] Charly Carrière,[**] Dimitri Mercier,[**] Sandrine Zanna,[**] and Philippe Marcus[‡,**]*

Two hybrid sol-gel coatings, one acrylate-based and the other epoxy-based, were synthesized and deposited on two cast aluminum-silicon alloys, Al-Si9-Cu3 and Al-Si7-Mg0.3. Field immersion testing was performed in the Adriatic Sea and lasted 8 months. Coatings were characterized before and after immersion in terms of morphology, structure, composition, and electrochemical properties in artificial seawater. The level of biofouling was documented, and sonication was used as a procedure for simulating vessels in motion or gentle cleaning. Although biofouling was formed during immersion, as analyzed by scanning electron microscopy, it was removed by sonication in a large proportion. X-ray photoelectron and glow discharge optical emission spectroscopies confirmed that the coatings preserved their structure and that no significant dissolution occurred. Both coatings showed better barrier properties when deposited on Al-Si7-Mg0.3 alloy and also exhibited the highest ability of biofouling release, making them good candidates for further development.

KEY WORDS: biocorrosion, biofouling, cast aluminum alloys, field testing, glow discharge optical emission spectroscopy, scanning electron microscopy, sol-gel coatings, x-ray photoelectron spectroscopy

INTRODUCTION

The use of aluminum alloys in marine environments is increasing due to the lightning trend of the vessels related to smaller fuel consumption. In Part 1 of this study, we investigated cast aluminum-silicon alloys for use in the marine environment.[1] Field testing lasting for 8 months showed that Al-Si9-Cu3 and Al-Si7-Mg0.3 withstood the chloride environment of seawater by forming a protective Al(III) oxide layer. The layer formed on Al-Si7-Mg0.3 alloy was especially protective, consisting of Al-oxide and Si grains in the eutectic regions. The oxide layers formed during immersion were a few micrometers thick. Although these cast alloys can withstand corrosive attacks in the marine environment, they are prone to biofouling. After 1 month of immersion, biofouling could be removed by sonication; however, after 8 months, macrofouling was firmly attached to the surface.[1] In practice, the presence of micro- and macrobiofouling at the vessel's surface represents a severe complication—it increases the surface roughness and friction, leading to a lower speed and increased fuel consumption. To combat this process, antifouling (AF) coatings are being used. The economic impact of biofouling is enormous: 40%-increased fuel consumption and estimated overall costs for transport delays, hull repair, cleaning, and general maintenance are 150 billion USD per year.[2] Thus, even modest improvements in the fouling conditions can save enormous financial means.

The AF coatings mainly consist of hydrophobic or superhydrophobic tensides based on organosilicon polymers carrying fluorine-based tails and metal biocide additives.[3] Both compounds, fluorine and metal biocides, cause environmental concerns and are toxic to a broad spectrum of marine organisms at specific levels. One of the most effective AF agents is organotin tributylin (TBT), which was banned or restricted by the International Maritime Organization in 2008 due to its high toxicity to a wide range of nontarget aquatic organisms and readily accumulation in them, posing a threat to human health through the digestion as food.[4] However, it seems that the use of TBT still persists.[5] It is now proven that even biocides alternative to toxic TBT are also environmentally hazardous—copper ions released from AF coatings account for 70% of total copper found in harbors; at specific levels, it is toxic to a broad spectrum of marine organisms from microalgae to vertebrates as fishes and mammals.[6] Many harbors forbid the mechanical underwater cleaning of ships painted with Cu-based coatings. Another biocide alternative to TBT is zinc pyrithione, which is also potentially harmful.[7] Environmental concerns even arise related to the use of coatings that do not exhibit biocidal activity but have, e.g., more than four $-CF_2$ units in the backbone due to their long-term persistence in the environment and permanent exposure.[8] There is a strong need to search for new alternatives which are efficient and environmentally benign.

Submitted for publication: September 15, 2022. Revised and accepted: December 1, 2022. Preprint available online: December 1, 2022, https://doi.org/10.5006/4206.
‡ Corresponding authors. E-mail: ingrid.milosev@ijs.si; philippe.marcus@chimieparistech.psl.eu.
* Jožef Stefan Institute, Department of Physical and Organic Chemistry, Jamova c. 39, Ljubljana, 1000, Slovenia.
** CNRS—Chimie ParisTech, PSL University, Institut de Recherche de Chimie Paris, Physical Chemistry of Surfaces Group, 11 rue Pierre et Marie Curie, Paris, 75005, France.

ISSN 0010-9312 (print), 1938-159X (online)

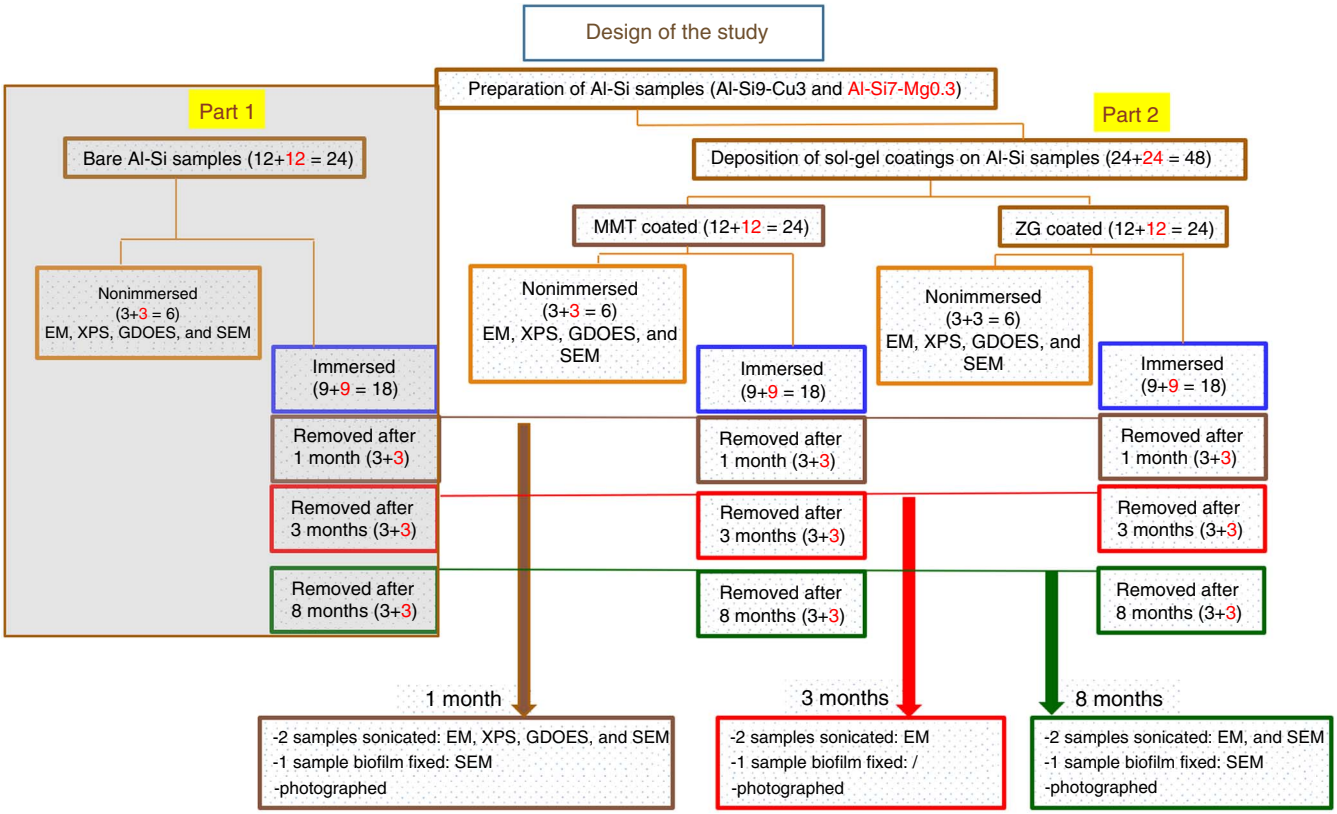

FIGURE 1. *Organigram presents the design of the study. EM—electrochemical measurements; XPS—x-ray photoelectron spectroscopy; SEM—scanning electron microscopy; and GDOES—glow discharge optical emission spectroscopy. The experiments presented in Part 1 of the study are shaded. The numbers of samples are given in parentheses.*

There are generally two approaches to combat biofouling:[9-15] (i) biocide-release AF coatings and (ii) nonbiocide release AF coatings. Biocide-release coatings apply the dispersion of biocide additive in polymer binders which then release biocide and kill attached microorganisms. They can be divided into insoluble or soluble matrices depending on whether the matrix progressively leaches only biocide agents or dissolves away with a biocide agent.

Nonbiocide-release AF coatings are more attractive than biocide coatings from an environmental point of view. They can be divided into two main strategies. The first strategy is the detachment of biofouling (so-called fouling-release principle), aiming to reduce the adhesion strength of settled organisms via hydrophobic interactions; settled organisms can be easily removed when exposed to hydrodynamic shear stress during ship movement. When the vessel is in movement, these poorly adhered organisms are removed due to shear stress. Polymers suitable for this category should have a flexible, linear backbone, low elastic modulus, closely-packed functional groups, and cross linkage among them. Two main groups are poly(siloxanes) and fluoropolymers. Poly(dimethylsiloxane) (PDMS) is used mainly due to low critical surface tension, roughness, and conformational mobility, allowing close packing. PDMS coatings can contain fillers of different natures: either inorganic to improve mechanical properties or organic-like poly(urethane) to achieve a microtopographic surface. Fluorine-based coatings exhibit low critical surface energy with nonsticking properties based on $-CF_3$ groups. Some commercial coatings are already based on the combined siloxane-fluorine-based coatings, e.g., Intersleek 900®[†], Hempasil X3®[†]. Their lifetime is 5 y to 10 y.

The second strategy is the prevention of attachment (so-called fouling-resistant principle), aiming to prevent adhesion and settlement of biofouling via hydrophilic interactions. The most used compound is poly(ethylene glycol) which creates a surface not favoring adsorption.[3] Other approaches include superhydrophobic surfaces, enzyme-based coatings, biomimetic topographic approaches, amphiphilic coatings, and sol-gel coatings.[9-15] The sol-gel coatings were used in this work to coat cast aluminum-silicon alloys aiming to field test them in marine environments. In our previous studies, we have synthesized several acrylate-[16-26] and epoxy-[27]based hybrid (inorganic-organic) sol-gel coatings for barrier protection of aluminum alloys[16-27] and structural steel[24] for protection in chloride environment[20-27] and simulated aircraft conditions.[17-19,22] The development of sol-gel coatings has progressed significantly in the last decade and reached the point when the tailoring of surface properties can be used for a broad spectrum of applications.[28-29] One of the possible applications is its use in the maritime environment.[15] Our recent field test study on acrylate-based coatings deposited on structural steel showed that sol-gel coatings represent a good basis for further development and incorporation as a topcoat in the full system, including primer and interlayer.[30] The current work presented here aimed to prepare two hybrid sol-gel formulations, one acrylate and the other epoxy-based, deposit them in the form of coatings on cast Al-Si9-Cu3 and Al-Si7-Mg0.3 alloys, and field test them in the Adriatic Sea. Before and after immersion

[†] Trade name.

for 8 months, samples were analyzed using different surface analytical methods and electrochemical measurements in artificial seawater. This study is, therefore, the continuation of Part 1.[1] The main focus was the corrosion protection and biofouling ability of sol-gel coatings. One of the issues of interest is whether these coatings can perform according to the fouling-release strategy.

EXPERIMENTAL PROCEDURES

2.1 | Substrate Material and Chemicals for Sol-Gel Syntheses

Two types of aluminum alloys, manufactured by Talum d.d. Kidričevo, Slovenia, were used as substrates: (1) Al-Si9-Cu3 alloy (380.0/EN AC[(1)]46000/EN AC Al-Si9-Cu3(Fe)/UNS[(2)] A0380) and (2) Al-Si7-Mg0.3 alloy (A356.0/EN AC 42100/EN AC Al-Si7-Mg0.3/UNS A13560). Their composition was given in Part 1. Samples were cut in the form of plates with dimensions 80 mm × 39 mm × 4 mm (Al-Si9-Cu3) and 80 mm × 34 mm × 4 mm (Al-Si7-Mg0.3). On each shorter side of the rectangle, a hole with a diameter of 3 mm was made for the fixation of the sample on the rack. Samples were then water-ground on both sides using SiC emery papers of 320 grit (LabPole-5[†], Struers, Ballerup, Denmark). In total, 48 bare samples were prepared and coated (24 of each alloy type, Figure 1).

The following chemicals were used for the synthesis of acrylate-based sol: tetrahydrofuran (THF, 99.9%, Sigma Aldrich), 3-(trimethoxysilyl)propyl methacrylate (MAPTMS, 98%, Aldrich), tetraethyl orthosilicate (TEOS, 99%, Aldrich), benzoyl peroxide (BPO, 97%, Alfa Aesar), methyl methacrylate (MMA, 99%, Aldrich), ethanol (99%), and acidic water (pH = 1). This acrylate-based sol was denoted MMT (abbreviation of MAPTMS +MMT+TEOS).

The following chemicals were used for the synthesis of epoxy-based sol: zirconium(IV) propoxide, (ZTP: $Zr(OPr)_4$, 70 wt%, in 1-propanol, Aldrich), (3-glycidyloxypropyl)trimethoxy silane (GPTMS, 98.0%, Aldrich), and acetic acid (AcOH, 100%, Appli-Chem). This epoxy-based sol was denoted ZG (abbreviation of ZTP+GMPTMS).

Alkoxide precursors and all reagents were used as received without further purification.

2.2 | Sol-Gel Synthesis and Deposition of the Coatings

The sol-gel synthesis and coating characterization was presented in detail in previous publications[16-25,27] and will be herein briefly presented (Figure S1). Sols/coatings were abbreviated according to the initials of the main precursors MMT and ZG, as explained in the previous section. All reactions were performed in a pilot laboratory reactor with a volume of 0.13 L.

MMT acrylate-based inorganic-organic hybrid sol was synthesized by mixing two separately prepared solutions (Figure S1). The preparation of the first sol (sol 1) started by dissolving BPO in THF at room temperature. A mixture of MMA and MAPTMS was added to the flask and heated under reflux for 4 h. The volume of THF was adjusted to obtain the coating with a thickness of about 3 μm. The reaction mixture was then allowed to cool to room temperature for 20 min. While cooling, the second sol (sol 2) was prepared from TEOS, ethanol, and water acidified to pH = 1 using nitric acid. The second sol was mixed with the first sol (sol 1 + sol 2) and stirred for 1 h to give the final sol used for deposition. The molar ratios of the chemical in the final sol were MAPTMS : TEOS : MMA : H_2O : BPO : EtOH = 1 : 2 : 8 : 10.5 : 0.08 : 5. Sol MMT was deposited on the substrate surface by a dip-coater (Bungard[†], RDC15). One layer was applied at an immersion time of 2 s and a withdrawal rate of 14 cm/min.

ZG epoxy-based inorganic-organic hybrid sol was synthesized in two steps by mixing two separately prepared solutions, sol 1 and sol 2 (Figure S1).[27] Sol 1 was prepared by mixing ZTP and acetic acid in the ratio 1:4. Water was then added in a 1:1 molar ratio (Zr:H_2O = 1:5). Sol 2 was made by mixing GPTMS with acetic acid in a 1:3 molar ratio. Water was then added immediately to a molar ratio of GPTMS to the water of 1:3. Each sol was stirred for 15 min and mixed under vigorous stirring at 300 rpm for 15 min to induce gelation, giving a hybrid ZG sol. During synthesis, each solution was stirred using a magnetic stirrer at a speed of 400 rpm. Sol ZG was deposited on the substrate surface by a dip-coater (Bungard, RDC15). One layer was applied at an immersion time of 2 s and a withdrawal rate of 14 cm/min.

After deposition, samples were heated up to 170°C (heating rate 3°C/min) and then maintained at this temperature for 1 h. The resulting MMT and ZG coatings were homogeneous and transparent when looked at with the naked eye.

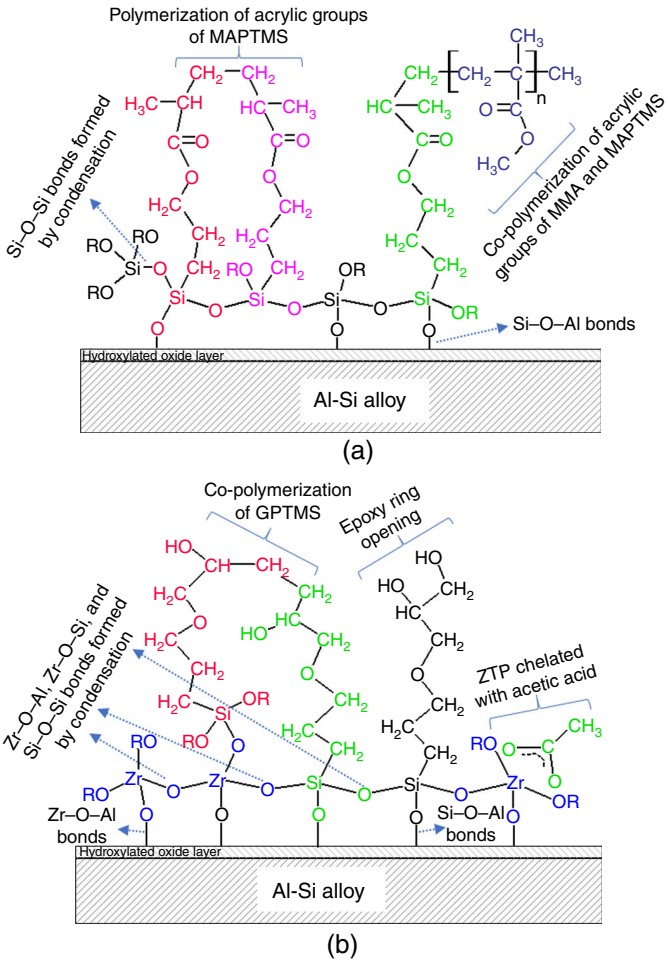

FIGURE 2. *Schematic presentation of the composition of sol-gel coating MMT and ZG deposited on Al-Si alloys.*

(1) EN = European Standards (German "Europäische Norm" EN), AC = Aluminum Cast

(2) UNS numbers are listed in *Metals & Alloys in the Unified Numbering System*, published by the Society of Automotive Engineers (SAE International) and cosponsored by ASTM International.

2.3 | Design of the Study

2.3.1 | Preparation of the Samples

Out of 24 coated samples of each alloy (Al-Si9-Cu3 and Al-Si7-Mg0.3), 12 were coated with MMT and 12 with ZG coatings (Figure 1). Out of 12 prepared samples of each alloy, three were not immersed in seawater but were used as benchmarks for the conditions before the testing in the Adriatic Sea. Electrochemical measurements, water contact angle, x-ray photoelectron spectroscopy (XPS), glow discharge optical emission spectroscopy (GDOES), and scanning electron microscopy (SEM) analyses were performed on these samples. Nine coated samples of each alloy type were immersed in the Adriatic Sea, three replicates of each immersion period (1, 3, and 8 months). Altogether 12 out of 48 coated Al-Si9-Cu3, and Al-Si7-Mg0.3 samples were used in nonimmersed conditions, and 36 samples were immersed. Samples were mounted on a specially designed rack (Part 1) to be taken out after 1, 3, and 8 months, respectively.

2.3.2 | Field Testing in the Adriatic Sea

The field testing procedure, conditions, sample removal, and treatment were the same as in Part 1.

2.3.3 | Treatment of the Immersed Samples

The procedure of field testing, conditions, sample removal, and preparation for the analyses were the same as in Part 1. The only difference is that electrochemical measurements were performed in at least three replicates on the samples immersed in the Adriatic Sea for 8 months as biofouling formed much less than on bare samples.

2.4 | Characterization Methods

The water contact angle was measured for the nonimmersed samples at room temperature by the static sessile-drop method on a Krüss FM40[†] Easy Drop contact-angle measuring system. A small water drop (4 µL) was formed on the end of the syringe and carefully placed on the surface. Digital images of the droplet silhouette were captured with a high-resolution digital camera, and the contact angle was determined by numerical fitting the droplet image using associated protocol software. The values reported the average of at least five measurements on randomly chosen sites (reported as mean±standard deviation).

All other characterization methods were described in Part 1.

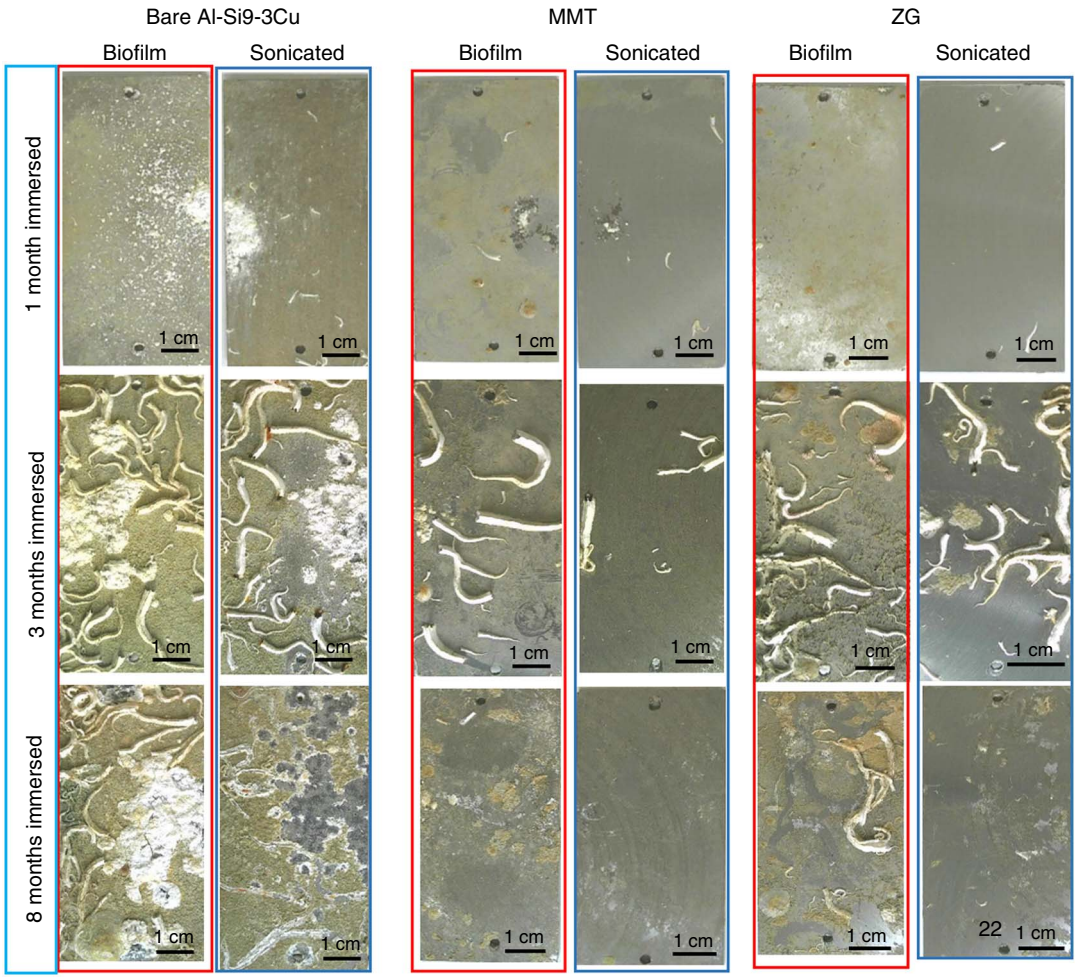

FIGURE 3. *Photos of Al-Si9-Cu3 samples coated with MMT and ZG coatings after 1, 3, and 8 months of immersion in the Adriatic Sea covered with biofilm and after removal of the biofilm by sonication. Photos of bare Al-Si9-Cu3 samples under the same conditions are given in the two first columns for comparison (already published in Figure 7 in Part 1).*

RESULTS AND DISCUSSION

3.1 | Sol-Gel Coatings

Two sol-gel coatings were tested on Al-Si9-Cu3 and Al-Si7-Mg0.3 substrates: acrylate-based MMT and epoxy-based ZG coatings. Both coatings are hybrid, i.e., contain an inorganic part of the sol-gel network and an organic, polymerized part of the network. Sols, later deposited in the form of coatings, were prepared by a sol-gel procedure, including hydrolysis and condensation reactions of siloxanes and organically modified siloxanes (Figure S1). The sol synthesis and characterization of the deposited coatings were presented in previous publications.[16-17,19,22,24]

The inorganic part of MMT coating, containing homogeneous (Si–O–Si) siloxane bonds, is mainly responsible for the coating's thermal stability, hardness, and durability (Figure 2[a]). Heterogenous (Si–O–Al) siloxane bonds achieve good adhesion to Al alloy. The organic part of the sol-gel is a polymerized acrylate network, which is intermixed with the inorganic part and contributes to the coating's density and toughness. Polymerizing acrylate groups form the acrylate network on both MAPTMS and MMA.[16-17,22] The thickness of MMT coating deposited by dipping on Al-Si9-Cu3 substrate was about 3 μm, as determined by SEM along the scribe (not shown).

The inorganic part of ZG coating contains condensed homogeneous (Zr–O–Zr) bonds and incorporates acetate in its structure in bidentate chelate coordination (Figure 2[b]). The hydrolysis of GPTMS leads to the formation of Si–O–Si siloxane bonds and, in the final sol, to Zr–O–Si bonds. During curing, polymerization of the organic part of the network occurred together with the opening of the epoxy ring, which is thermally initiated.[27] Acetate incorporated in the sol eventually evaporated. The thickness of the ZG coating deposited by dipping was about 3 μm, as determined by SEM along the scribe.

After grinding, the water contact angle (WCA) of bare Al-Si9-Cu3 was 21°. The coatings increased the WCA to 77° for MMT and 99° for ZG coatings. WCA of bare Cu-Si7-Mg0.3 was 45°. The coatings increased the WCA to 81° for MMT and 85° for ZG coatings. The coated surfaces thus become more hydrophobic (larger WCA) than bare ones, implying smaller surface wettability.

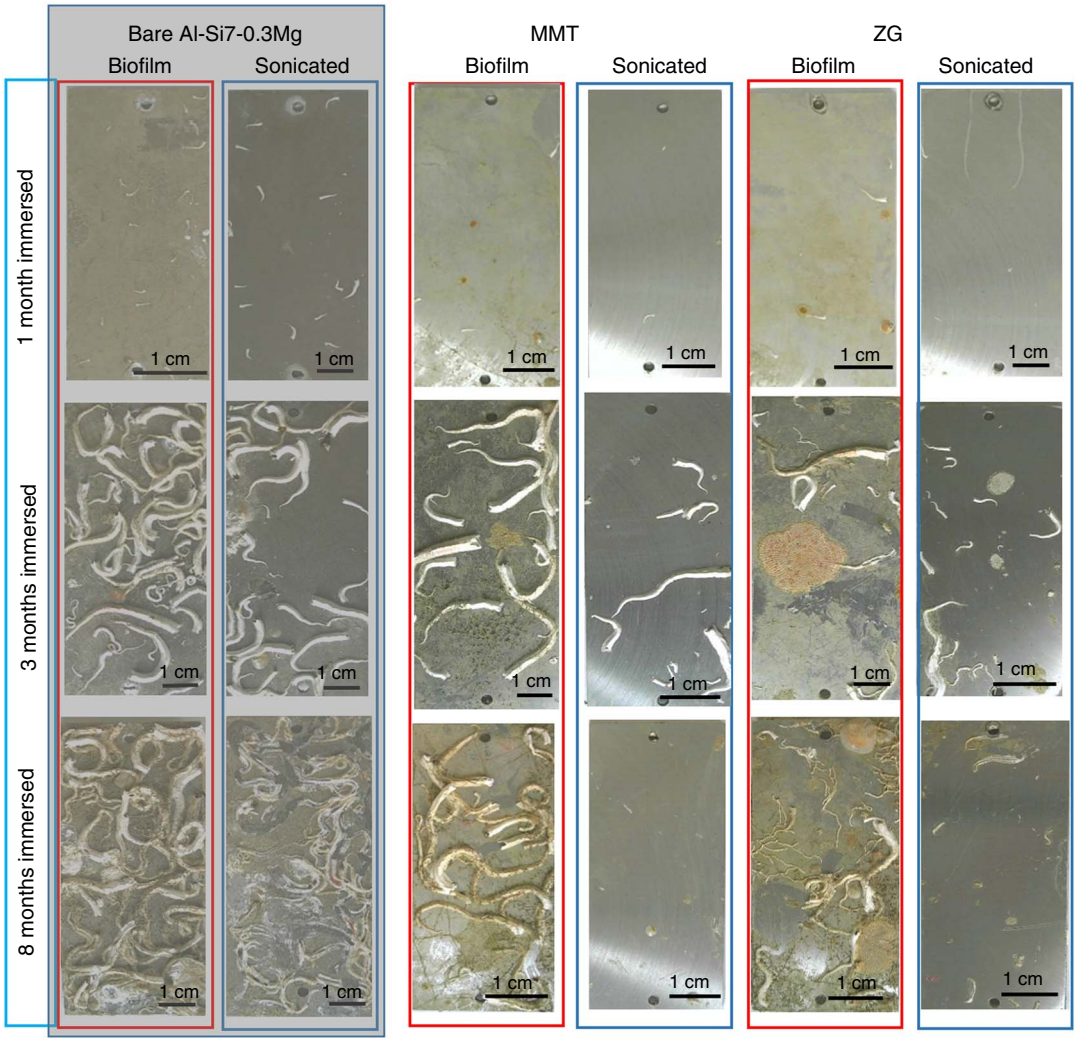

FIGURE 4. *Photos of Al-Si7-Mg0.3 samples coated with MMT and ZG coatings after 1, 3, and 8 months of immersion in the Adriatic Sea covered with biofilm and after removal of the biofilm by sonication. Photos of bare Al-Si7-Mg0.3 samples under the same conditions are given in the two first columns for comparison (already published in Figure 7 in Part 1).*

3.2 | Images of Samples Before and After Immersion in Seawater

Images of racks with Al-Si9-Cu3 and Al-Si7-Mg0.3 samples before and after 1, 3, and 8 months of immersion in the Adriatic Sea are presented in Figures S2 and S3. The progressive coverage of samples with biofouling and attached microorganisms is evident during prolonged immersion.

Individual samples after immersion for 1, 3, and 8 months are presented in Figures 3 and 4. Samples were imaged before and after sonication. The attachment of biofouling (biofilm) and microorganisms is especially pronounced on bare samples (presented in Part 1), whereas there was considerably less attached biofouling on both coated samples. The amount of biofouling increased with increasing immersion time. After 1 month of immersion, the surface of coated samples was covered by brownish layers of microbiofouling; those could be easily detached by sonication, and the coated samples regained a shiny appearance due to the removal of biofouling. Sonication was used as a procedure simulating vessels in motion or a simple mechanical cleaning step. Almost no mesoscale biofilm formation was noticed after this immersion period. After 3 and 8 months of immersion, sonication could still remove larger microorganisms and attached biofouling, opposite to bare samples where the foul and microorganisms remained firmly attached to the surface.

3.3 | Scanning Electron Microscopy Analysis of Coated Substrates Before and After Immersion in Seawater

SEM images of coated Al-Si9-Cu3 and Al-Si7-Mg0.3 samples before immersion in the Adriatic Sea are presented in Figure 5. Both coatings show a homogeneous and dense structure (with occasional surface defects). High-magnification images in insets show the nanostructured morphology of the coatings.

3.3.1 | Al-Si9-Cu3 Coated Samples

SEM images of both biofouling-covered and sonicated conditions recorded after immersion are presented in Figure 6 for the Al-Si9-Cu3 samples coated with MMT and ZG coatings (magnification 5,000×). Images recorded at a magnification of 1,000× are presented in Figure S4, together with that of the nonimmersed sample. After 1 month of immersion, the bare sample was covered by a thick layer of biofouling (mainly diatoms), which was removed by sonication, revealing a compact surface layer formed during immersion (Figures S4[b] and [c]). After sonication, the biofouling was almost wholly removed, revealing that the underlying coating was still virtually intact, as observed in the inset image at a high magnification of 30,000× (Figure 6[b]). The ZG-coated surface was similar to MMT but showed larger diatoms attached to the surface (Figures 6[c] and S4[d] through [i]). After sonication, biofouling was almost completely removed, and the coating structure was preserved (Figure 6[d]).

SEM images after 8 months show the increased amount of biofouling and more than 10 μm large diatoms (Figures 6[e] through [h]). Despite the presence of such large microorganisms, the sonication was efficient in removing the biofouling revealing the intact structure of the underlying coating. SEM images recorded at smaller magnifications are presented in Figure S5.

3.3.2 | Al-Si7-Mg0.3 Coated Samples

SEM images of both biofouling-covered and sonicated conditions recorded are presented in Figure 7 for the Al-Si7-Mg0.3 samples coated with MMT and ZG coatings (magnification 5,000×). Images recorded at a magnification of 1,000 × are presented in Figure S6, together with that of the nonimmersed sample. After 1 month of immersion, the bare sample was

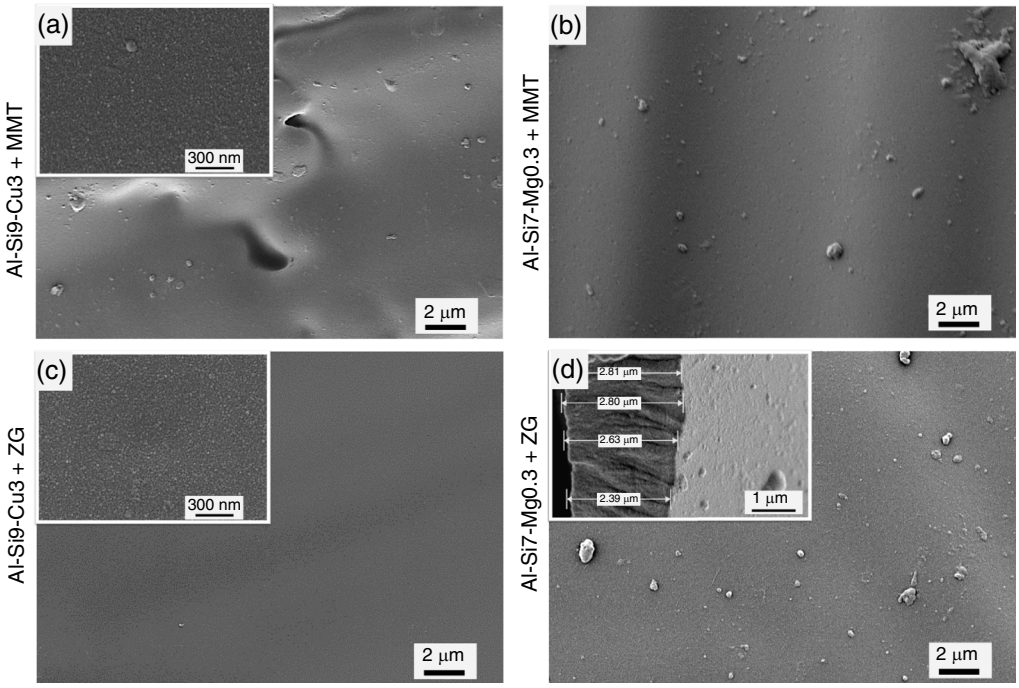

FIGURE 5. *SEM images (SE mode) of the coated Al-Si9-Cu3 and Al-Si7-Mg0.3 samples before immersion: (a) Al-Si9-Cu3 coated with MMT, (b) Al-Si7-Mg0.3 coated with MMT, (c) Al-Si9-Cu3 coated with ZG, and (d) Al-Si7-Mg0.3 coated with ZG. Inset in (d) is made at the cross section. Magnification 5,000×, 15 kV.*

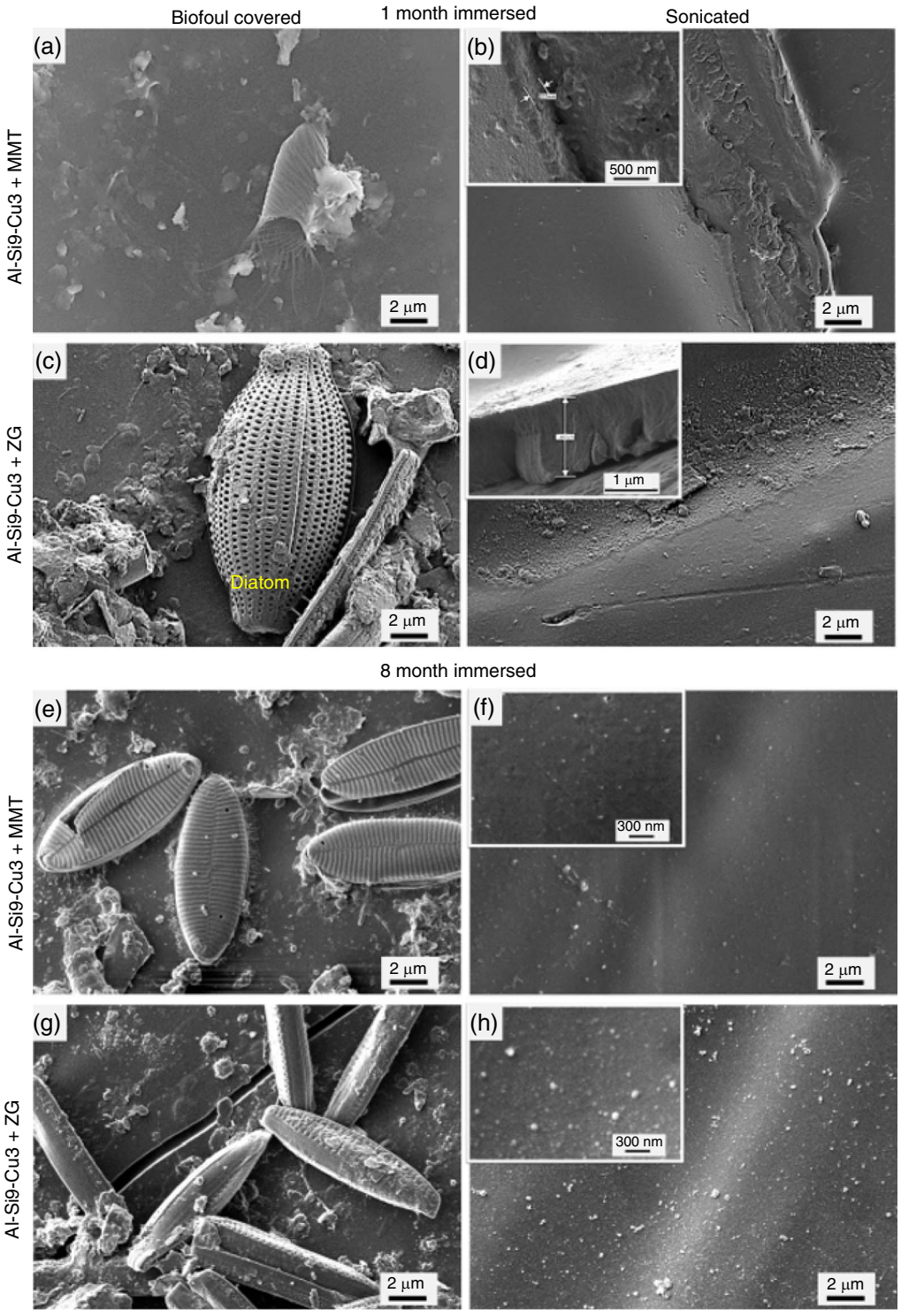

FIGURE 6. *SEM images (SE mode) of the coated Al-Si9-Cu3 samples after immersion for (a) through (d) 1 month and (e) through (h) 8 months in the Adriatic Sea. Images taken at the biofoul-covered samples are in the right column (a, c, e, and g). Images taken at the samples after sonication and removal of biofoul are in the left column (b, d, f, and h). Magnification 5,000×, 15 kV. SEM images recorded for nonimmersed and immersed samples at a magnification of 1,000× after immersion of 1 month and 8 months are given in Figures S4 and S5, respectively.*

covered by a thick biofouling layer. The example of diatoms is presented in the inset in Figure 7(a). Biofouling was removed by sonication, revealing a compact surface layer formed during immersion (Figures S6[b] and [c]). After sonication, the biofouling was almost completely removed, revealing that the underlying coating was still virtually intact. The coated samples behave similarly (Figures 7[c] and S6[e] through [i]). After sonication, biofouling was almost completely removed, and the coating structure was preserved.

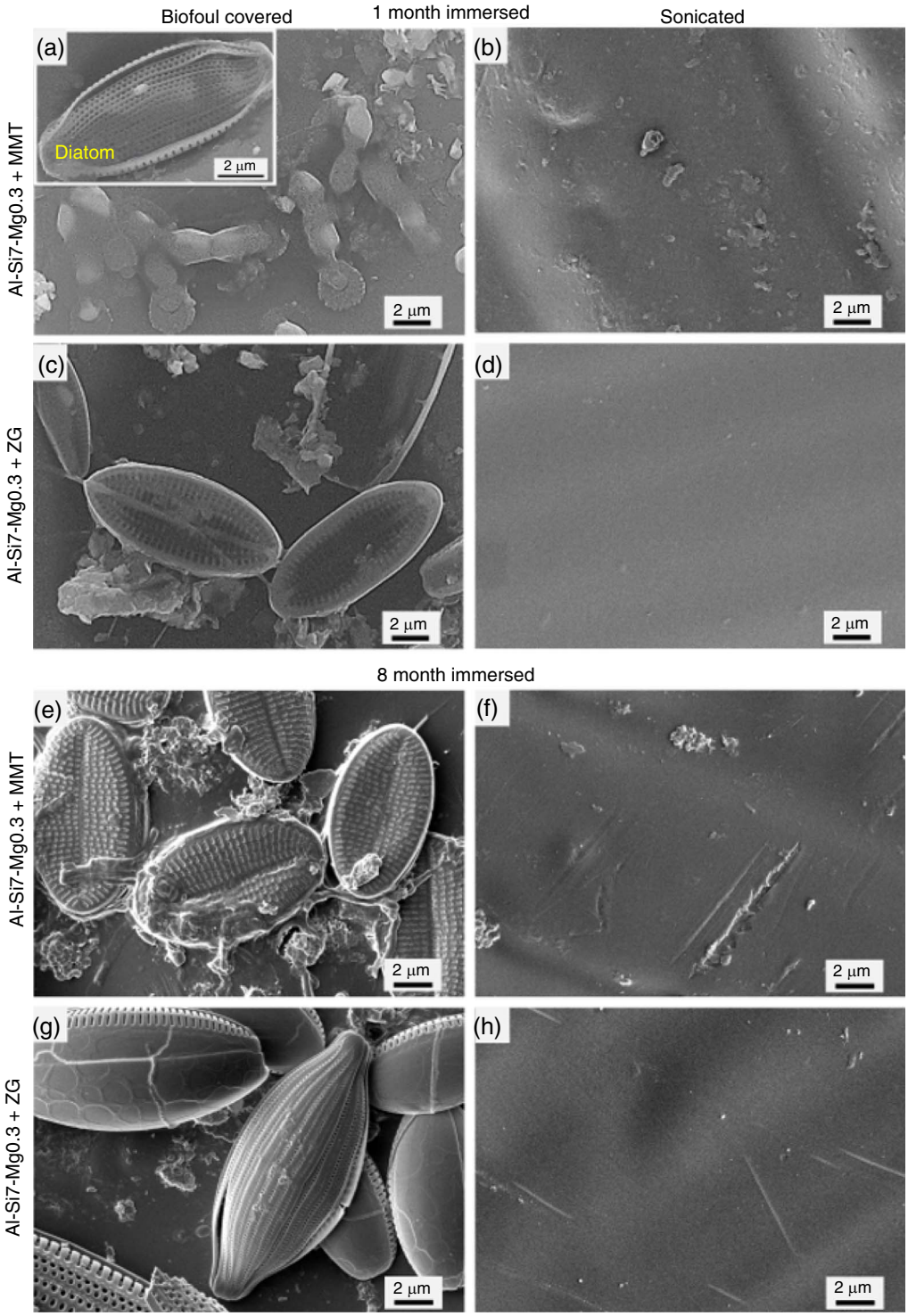

FIGURE 7. *SEM images (SE mode) of the coated Al-Si7-Mg0.3 samples after immersion for (a) through (d) 1 month and (e) through (h) 8 months in the Adriatic Sea. Images taken at the biofoul-covered samples are in the right column (a, c, e, and g). Images taken at the samples after sonication and removal of biofoul are in the left column (b, d, f, and h). Magnification 5,000×, 15 kV. SEM images recorded for nonimmersed and immersed samples at a magnification of 1,000× after immersion of 1 month and 8 months are given in Figures S6 and S7, respectively.*

SEM images after 8 months show the increased amount of biofouling and more than 10 µm large diatoms (Figures 7[e] through [h]), which were removed by sonication. SEM images recorded at smaller magnifications are presented in Figure S7.

3.4 | X-Ray Photoelectron Spectroscopy Analysis Before and After Immersion in Seawater

3.4.1 | Al-Si9-Cu3 Coated Samples

XPS survey spectrum for nonimmersed, MMT-coated Al-Si9-Cu3 (Figure S8) completely differs from the bare sample

(Part 1, Figure S7). The composition of the coating deduced from the spectra is given in Table 1. The coating is mainly organic and contains almost 67 at% C, 6.4 at% Si, and 26 at% O. The C/Si and O/Si are 10.4 and 4.1. Aluminum is detected in less than 0.5 at%. As only elements related to the hybrid MMT coating were detected (Si, C, and O), the coating is homogeneous and dense and therefore able to act as a barrier. Some minor elements (Cl and Ca) were also detected, probably related to the contamination from the chemicals used in sol-gel synthesis. High-resolution spectra are shown in Figure 8. The Si2p spectrum shows a single peak at 103.4 eV related to the formation of Si–C–Si and Si–O–Si bonds. The oxygen peak is located at 531.0 eV. The C1s spectrum is composed of more carbon species than the bare sample (Part 1, Figure S8), which reflects the presence of different organic species of polymerized acrylate network of MMT coating (Figure 2).

Table 1. *The Composition Deduced from the XPS Spectra Recorded at the Surface of Al-Si9-Cu3 Samples Coated with MMT Coating Before and After Immersion for 1 Month in the Adriatic Sea*[(A)].

	Composition (at%)	
Elements	**Before Immersion**	**After Immersion**
Al	0.4	1.6
Si	6.4	5.4
C	66.7	60.6
O	26.5	32.4

[(A)] Related survey and high-energy resolution spectra are presented in Figures S8 and 8, respectively.

Survey spectra recorded on immersed sample after sonication are quite similar to that of the nonimmersed sample (Figure S8). However, a small difference can be observed: Al was detected in the concentration of 1.6 at%, ca. four-fold compared to the initial concentration (Table 1). This is better observable in high-energy resolution spectra (Figure 8); a single peak appears at 74.4 eV, indicating the formation of Al(III) oxide/hydroxide. Because Si is an alloying element of the substrate and the coating element, it is difficult to differentiate whether some Si originating from the substrate is present on the coating surface. No other alloying element (Cu and Zn) could be detected.

Nonetheless, the presence of Al on the immersed coated sample suggests that Al from the substrate was able to penetrate through the coating (as will be shown by electrochemical measurements below). The C/Si ad O/Si ratios changed during immersion to 11.2 and 6, respectively, suggesting a reduced Si content at the sample surface. The intensity of the Cl2p peak was similar to that before the immersion, indicating that it originates from contaminations from chemicals and is not due to the incorporation of chloride from seawater. A similar observation is valid for the N1s spectrum, which remained similar to the nonimmersed sample and is probably due to some contamination and not to the remaining traces of biofouling (Figure 8).

XPS survey spectrum of nonimmersed and immersed, ZG-coated Al-Si9-Cu3 sample is presented in Figure S9, and the composition is presented in Table 2. The spectrum is similar to that of MMT-coated samples except that, in addition to Si, C, and O, it also contains zirconium, following Si/Zr-based coating composition (Figure 2). No elements originating from the substrate were detected. The C/Si, O/Si, and Zr/Si are 9.4, 5.6, and 0.5, respectively. Some minor elements (N, Ca) were detected,

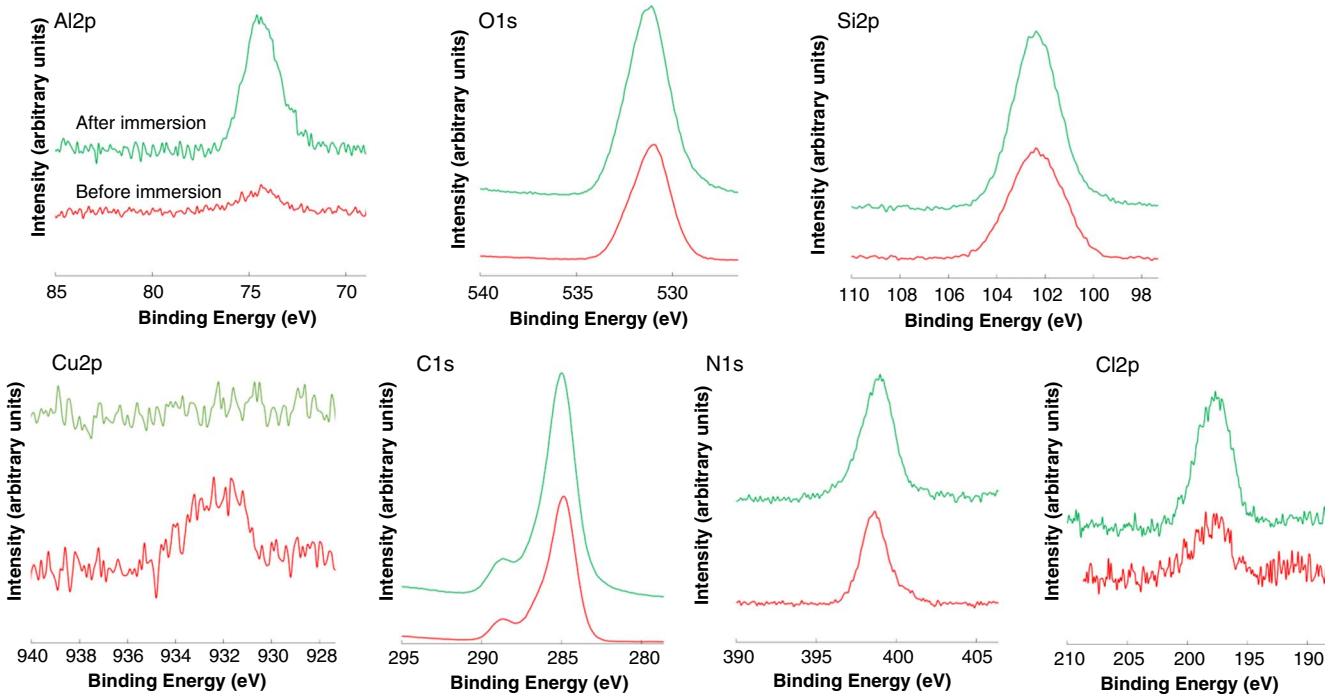

FIGURE 8. *XPS high-resolution spectra recorded at the surface of Al-Si9-Cu3 sample coated with MMT coating before and after immersion for 1 month in the Adriatic Sea. Related survey spectra are presented in Figure S8, and the composition is in Table 1. The samples were sonicated before the analysis.*

Table 2. *The Composition Deduced from the XPS Spectra Recorded at the Surface of Al-Si9-Cu3 Samples Coated with ZG Coating Before and After Immersion for 1 Month in the Adriatic Sea*[(A)]

Elements	Composition (at%)	
	Before Immersion	After Immersion
Al	–	0.8
Mg	–	0.7
Si	6.0	2.9
Zr	3.2	1.1
C	57.0	65.7
O	33.8	28.8

[(A)] Related survey and high-energy resolution spectra are presented in Figures S9 and 9, respectively.

probably related to the contamination from the chemicals used in sol-gel synthesis.

High-resolution spectra are presented in Figure 9. The silicon peak seems broader compared to that of MMT-coated samples. The Zr3d spectrum shows $3d_{5/2}$ and $3d_{3/2}$ peaks at 183.0 eV and 185.3 eV, indicating the formation of Zr(IV) oxide. XPS analysis thus confirms the coating structure schematically presented in Figure 2.

After immersion and sonication, some differences were observed: the C/Si and O/Si ratios increased during the immersion period (indicating some dissolution of silicon from the coating surface, as observed for MMT). The Zr/Si ratio was reduced to 0.4. The Al2p peak was detected after immersion (0.8 at%, see Table 2). Binding energies associated with the Si2p and Zr3d spectra remained virtually unchanged after the immersion, indicating preserved coating structure, as confirmed by SEM images (Figures 6 and S6).

3.4.2 | Al-Si7-Mg0.3 Coated Samples

XPS survey spectra for the MMT-coated Al-Si7-Mg0.3 samples, as prepared and immersed in the Adriatic Sea, are presented in Figure S10. The composition deduced from the spectra is given in Table 3. The as-prepared coated sample consists of Si, O, and C; only a small amount of Al was detected. The ratios C/Si and O/Si were 12.9 and 5.4, indicating high carbon content in the coating related to the polymerized acrylic network. High-resolution spectra in Figure 10 show that the Si2p peak is centered at 103.2 eV, indicating that siloxane is the main constituent of the coating.

After 1 month of immersion, the ratios C/Si and O/Si were 22.2 and 7.9, indicating some reduction of Si in the coating or enrichment with C and O (Table 3). Binding energies associated with the Si2p, C1s, and O1s spectra remained virtually unchanged by immersion, indicating a preserved coating structure (Figure 7). Also, the intensity of Al2p and Mg2p peaks did not increase, reflecting that no significant dissolution of substrate elements occurred through the coating.

Table 3. *The Composition Deduced from the XPS Spectra Recorded at the Surface of Al-Si7-Mg0.3 Samples Coated with MMT Coating Before and After Immersion for 1 Month in the Adriatic Sea*[(A)]

Elements	Composition (at%)	
	Before Immersion	After Immersion
Al	1.2	0.9
Si	5.1	3.2
C	65.8	70.7
O	27.9	25.2

[(A)] Related survey and high-energy resolution spectra are presented in Figures S10 and 10, respectively.

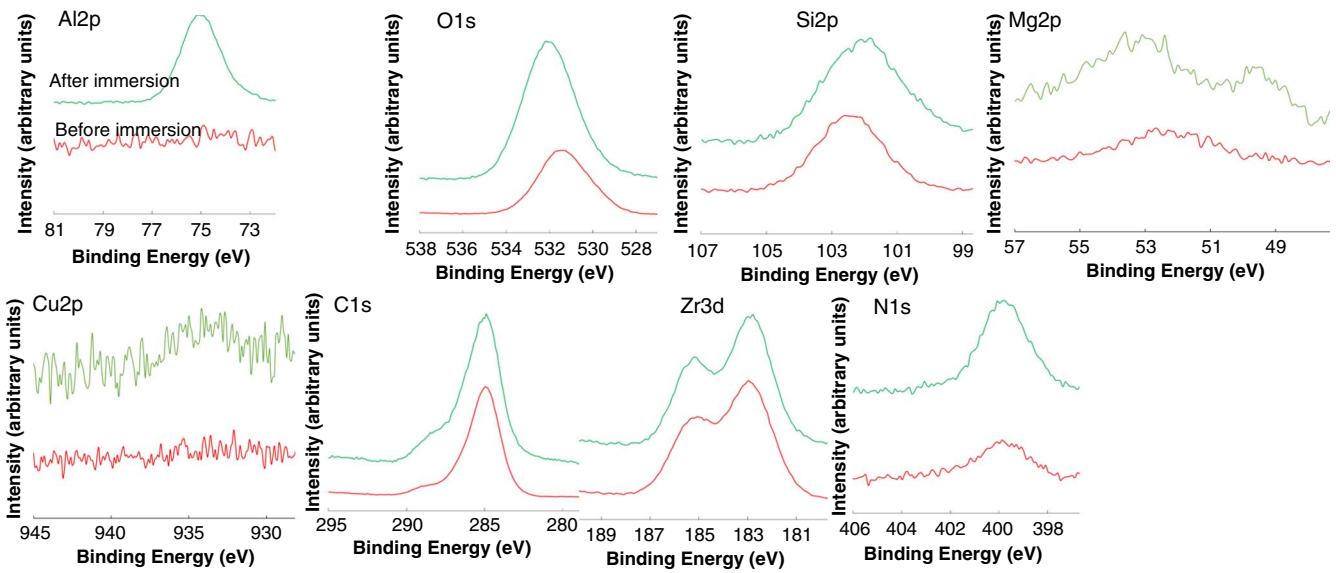

FIGURE 9. *XPS high-resolution spectra recorded at the surface of Al-Si9-Cu3 sample coated with ZG coating before and after immersion for 1 month in the Adriatic Sea. Related survey spectra are presented in Figure S9, and the composition is in Table 2. The samples were sonicated before the analysis.*

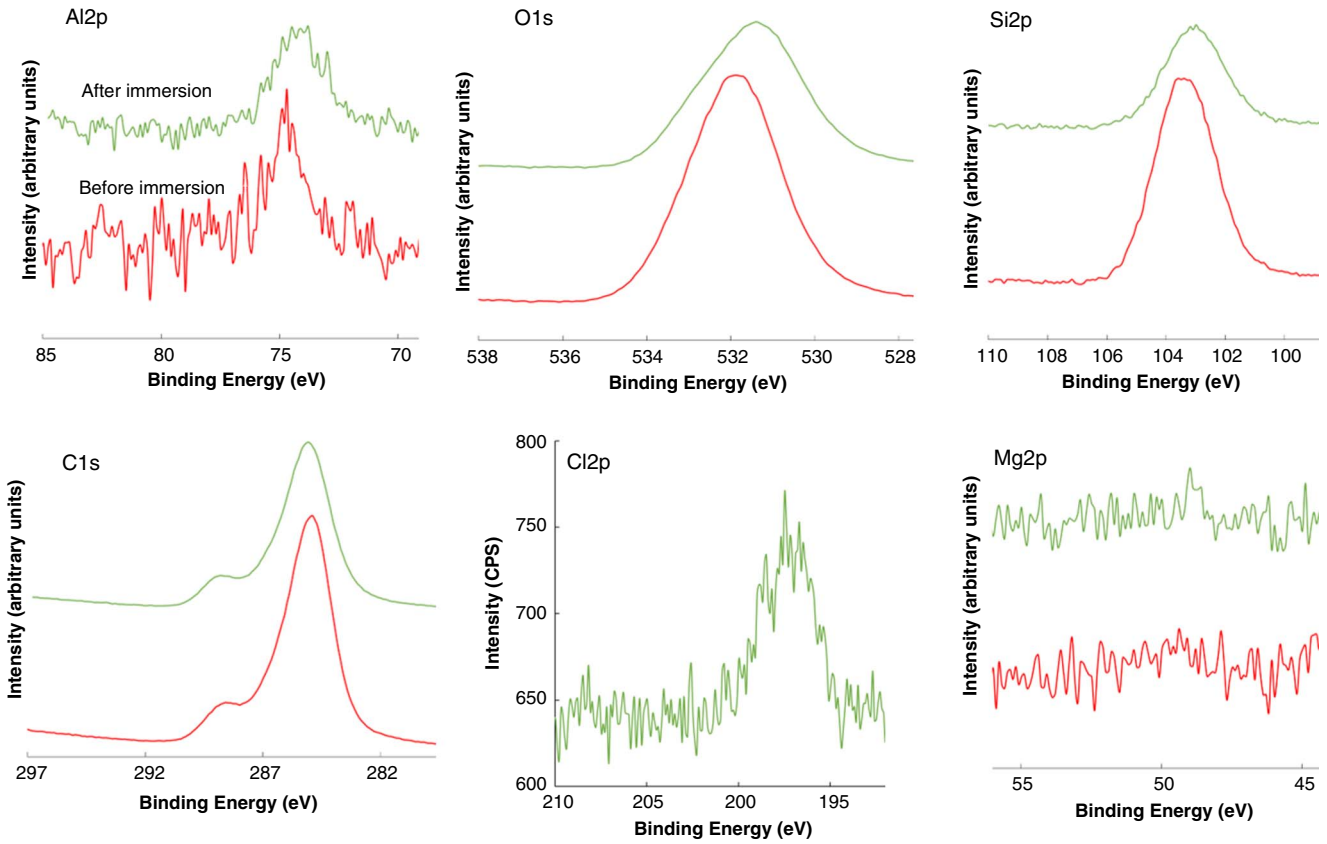

FIGURE 10. *XPS high-resolution spectra recorded at the surface of Al-Si7-Mg0.3 sample coated with MMT coating before and after immersion for 1 month in the Adriatic Sea. Related survey spectra are presented in Figure S10, and the composition is in Table 3. The samples were sonicated before the analysis.*

XPS survey spectra for ZG-coated Al-Si7-Mg0.3 samples, as prepared and immersed in the Adriatic Sea, are presented in Figure S11. The composition deduced from the spectra is given in Table 4. The coating consists of Si, O, C, and Zr showing C/Si, O/Si, and Si/Zr ratios of 17.9, 6.6, and 0.7, respectively. High-resolution spectra are presented in Figure 11 and are similar to those on Al-Si9-Cu3 (Figure 9). The intensity of Al2p and Mg2p peaks is small.

Table 4. *The Composition Deduced from the XPS Spectra Recorded at the Surface of Al-Si7-Mg0.3 Samples Coated with ZG Coating Before and After Immersion for 1 Month in the Adriatic Sea*[(A)]

	Composition (at%)	
Elements	**Before Immersion**	**After Immersion**
Al	0.8	–
Mg	2.0	–
Si	3.7	1.5
Zr	2.5	1.0
C	66.4	80.4
O	24.5	17.1

[(A)] Related survey and high-energy resolution spectra are presented in Figures S11 and 11, respectively.

After immersion, the ratios C/Si and O/Si increased strongly; however, no major change was observed in the shape of Si2p, O1s, and Zr3d spectra, indicating the preserved coating structure.

3.5 | Glow Discharge Optical Emission Spectroscopy Analysis After Immersion in Seawater

GDOES depth profiles of 1-month immersed and sonicated coated Al-Si9-Cu3 and Al-Si7-Mg0.3 samples are presented in Figures 12 and 13.

3.5.1 | Al-Si9-Cu3 Coated Samples

The GDOES profiles for the Al-Si9-Cu3 samples coated with ZG and MMT coatings after immersion for 1 month are presented in Figure 12. Only the profiles obtained after immersion are shown to simplify the figures. The general shape before immersion shows the coating layer (following the C signal). Compared to uncoated alloy (see Part 1, Figure 16), the elements of the underlying substrate were not presented but only the elements that originated from the coating (Si and C). The evolution of the C signal can be used as a marker of the coating layer. Assuming that the nature of the coating does not modify the sputtering rate, it is possible to conclude that the ZG coating is somewhat thicker than the MMT coating (~50 s and ~20 s for ZG and MMT coatings, respectively).

The two coatings show different behaviors with enrichment of Mg at the surface for MMT and localization of Mg in the coating for ZG. Na is mainly located in the coating. In contrast

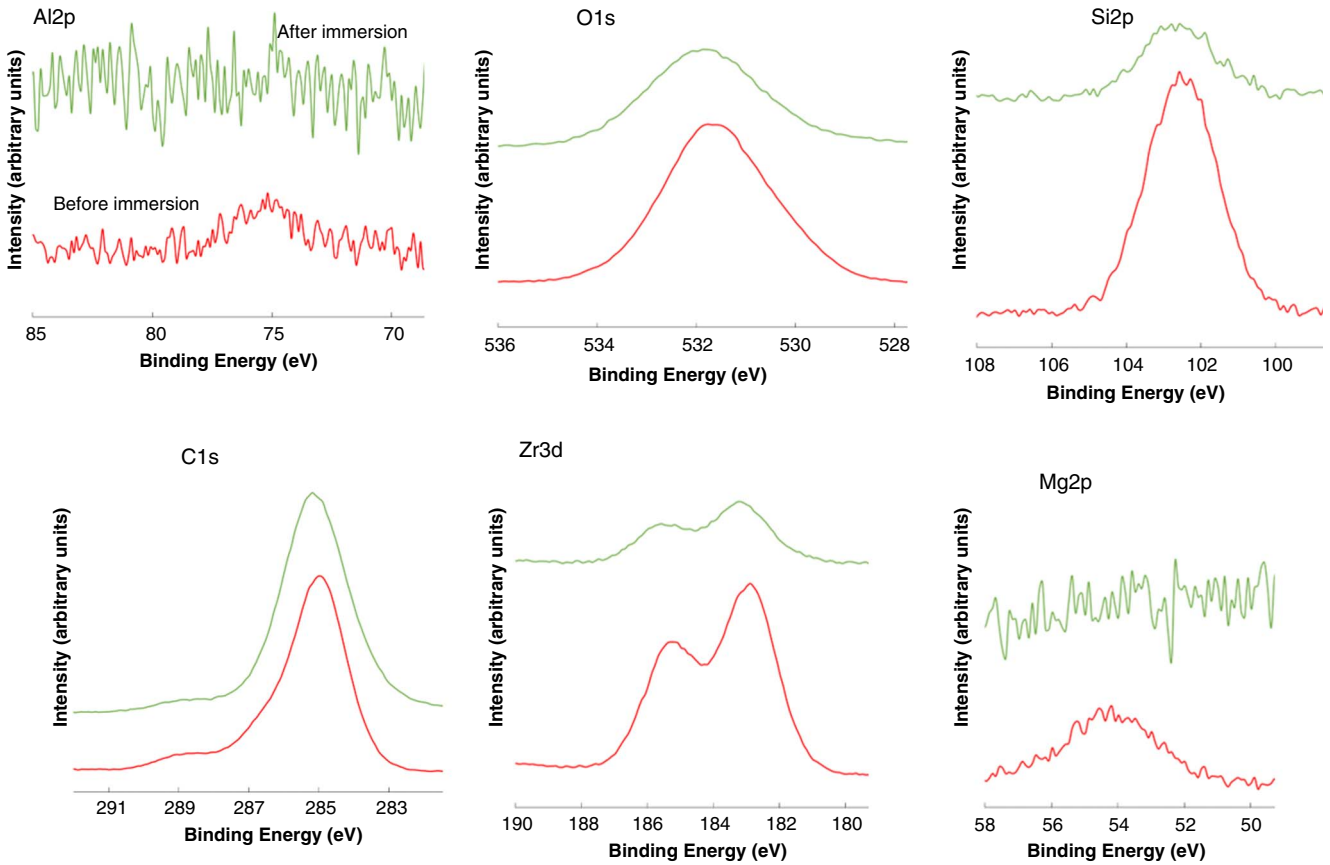

FIGURE 11. *XPS high-resolution spectra recorded at the surface of Al-Si7-Mg0.3 sample coated with ZG coating before and after immersion for 1 month in the Adriatic Sea. Related survey spectra are presented in Figure S11, and the composition is in Table 4. The samples were sonicated before the analysis.*

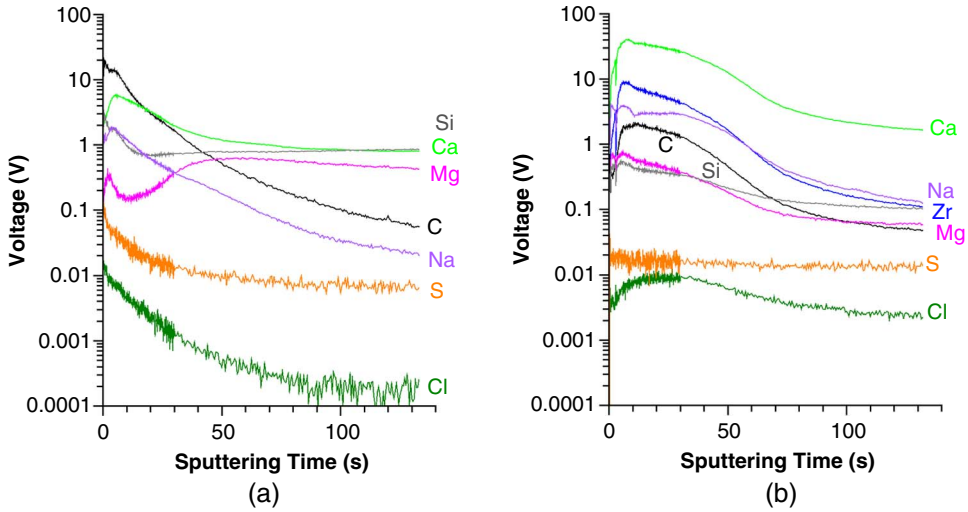

FIGURE 12. *GDOES depth profiles recorded at the surface of Al-Si9-Cu3 sample coated with (a) MMT coating and (b) ZG coating after immersion for 1 month in the Adriatic Sea.*

to uncoated alloys (see Part 1, Figure 16), no enrichment of Ca and Na is observed at the coating/metal interface, indicating that both coatings limit the diffusion of cations to the metal.

Cl is also present in both coatings, but no enrichment is observed at the coating/metal interface that could affect the corrosion resistance of the alloy.

3.5.2 | Al-Si7-Mg0.3 Coated Samples

Similar GDOES depth profiles have been performed for Al-Si7-Mg0.3 coated samples (Figure 13). After immersion, no significant change is observed on the general depth profiles (for Al, Si, and C), indicating that the corrosion process has not progressed for these coated alloys.

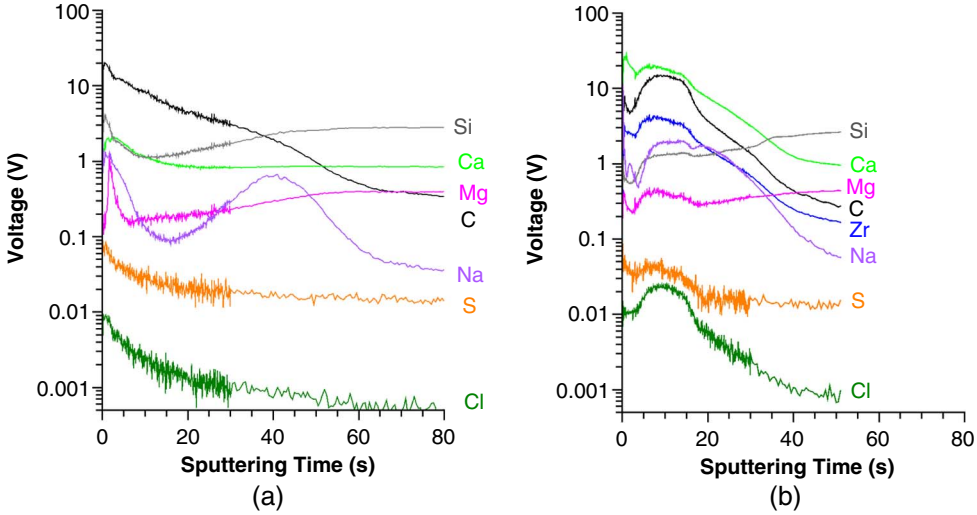

FIGURE 13. *GDOES depth profiles recorded at the surface of Al-Si7-Mg0.3 sample coated with (a) MMT coating and (b) ZG coating after immersion for 1 month in the Adriatic Sea.*

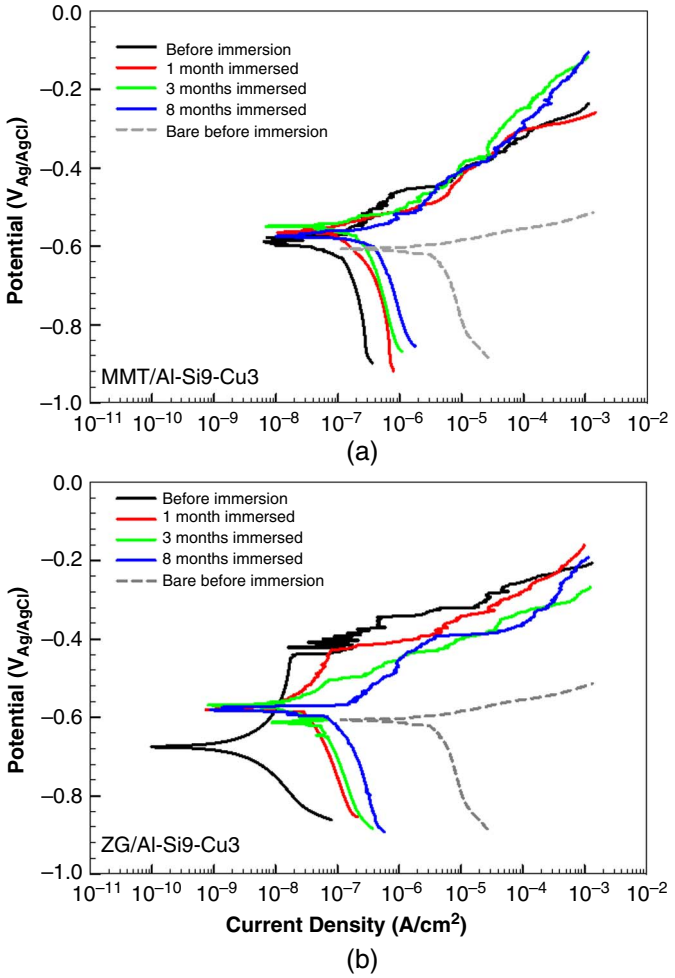

FIGURE 14. *Potentiodynamic polarization curves recorded in artificial seawater for Al-Si9-Cu3 coated with (a) MMT and (b) ZG coatings before immersion in the Adriatic Sea and after 1, 3, and 8 months of immersion. Before electrochemical measurements, the samples were sonicated to remove the biofilm formed during immersion in the seawater. The electrochemical parameters deduced from potentiodynamic curves are presented in Table 5. Curves for bare, nonimmersed samples are given for comparison.*

Table 5. *The Electrochemical Parameters Deduced from the Potentiodynamic Polarization Curves (Figure 14) Recorded for Al-Si9-Cu3 Samples Coated with MMT and ZG Coatings Before and After Immersion for 1, 3, and 8 Months in the Adriatic Sea*[A]

Condition	E_{corr} (V)	j_{corr} ($\mu A/cm^2$)	R_p ($k\Omega \cdot cm^2$)	E_{br} (V) (ΔE [mV])
Al-Si9-Cu3				
Before immersion	−0.61±0.02	2.97±0.24	3.5±1.6	−0.62 V (10 mV)
1 month immersed	−0.59±0.01	5.23±1.40	3.0±0.7	−0.44 V (150 mV)
3 months immersed	−0.56±0.01	2.77±0.51	3.0±0.1	−0.43 V (130 mV)
8 months immersed	−0.57±0.02	9.98±0.51	2.0±0.1	−0.38 V (190 mV)
Al-Si9-Cu3/MMT				
Before immersion	−0.60±0.01	0.13±0.07	567±193	−0.46 V (140 mV)
1 month immersed	−0.61±0.04	0.08±0.02	151±37	−0.42 V (190 mV)
3 months immersed	−0.58±0.03	0.26±0.06	165±134	−0.40 V (180 mV)
8 months immersed	−0.53±0.04	0.30±0.14	186±112	−0.39 V (140 mV)
Al-Si9-Cu3/ZG				
Before immersion	−0.64±0.03	0.003 ±0.001	6,043 ±1613	−0.44 V (200 mV)
1 month immersed	−0.58±0.03	0.03±0.01	1,039±196	−0.43 V (150 mV)
3 months immersed	−0.58±0.03	0.04±0.01	395±185	−0.44 V (140 mV)
8 months immersed	−0.57±0.02	0.14±0.07	213±144	−0.39 V (180 mV)

[A] The samples were sonicated before the analysis. The results for bare samples are given for comparison (already presented in Table 8 in Part 1).

For the elements from seawater (Mg, Cl, and Ca), the evolutions are similar to those observed for the coated Al-Si9-Cu3 showing the presence of Mg, Cl, and Ca in the coating. The only difference is the presence of Na at the coating/metal interface for the MMT coating. This observation could suggest the growth of an inorganic layer at this interface, as already observed on the uncoated alloys (at the oxide/metal interface) (see Part 1, Figure 18).

Similarly to the Al-Si9-Cu3 alloy, the presence of the two coatings significantly limits the corrosion process compared to the effects observed in Part 1 on this alloy, probably slowing down the diffusion of the species.

3.6 | Electrochemical Measurements Before and After Immersion in Seawater

3.6.1 | Al-Si9-Cu3 Coated Samples

The Al-Si9-Cu3 samples coated with MMT coating show a considerably better electrochemical response in artificial seawater than the bare sample (Figure 14[a], Table 5). The cathodic current density was smaller for ca. two orders of magnitude, reaching E_{corr} at –0.60 V. j_{corr} dropped from 2.97 μm/cm^2 to 0.13 μm/cm^2 and R_p increased from 3.5 kΩ·cm^2 to 567 kΩ·cm^2. In the anodic range, a passive domain was established, in contrast to the bare sample. The passive range was limited by the breakdown potential E_{br} at –0.46 V, giving a passive range of 140 mV ($|\Delta E = E_{br} - E_{corr}|$). EIS measurements performed at the open-circuit potential (E_{ocp}) are presented in Figure 15[a]. Significant improvements in electrochemical characteristics of the MMT coated sample compared to bare (Part 1, Figure 19) are reflected in the EIS measurements as well: |Z| was higher in the whole f range, reaching almost two orders of magnitude larger values at the lowest f (Figures 15[a] and [b]).

The curves recorded after immersion in the Adriatic Sea reflect relatively good stability of the MMT coating: the E_{corr} values were not significantly changed. However, the current density values measured were considerably smaller, and those of R_p larger than those of bare and ΔE increased (Part 1, Figure 19), i.e., the MMT coating still protected the substrate. Similar conclusions can be drawn from EIS measurements with |Z| decreasing in the whole f range, reaching 10^5 Ω·cm^2 at the lowest f (Figures 15[a] and [b]), with no considerable differences after 3 and 8 months of immersion.

The polarization curves recorded for the Al-Si7-Cu3 sample coated with ZG coatings are presented in Figure 14(b). ZG coating showed a more extensive passive range than MMT, with current densities dropping by three orders of magnitude (Table 5) compared to bare alloy (Part 1, Figure 19). The passive region was established with current density in the 0.01 μm/cm^2 range extending up to E_{br} at –0.44 V, resulting in ΔE of 200 mV (Figure 14[b]). EIS response was similar to

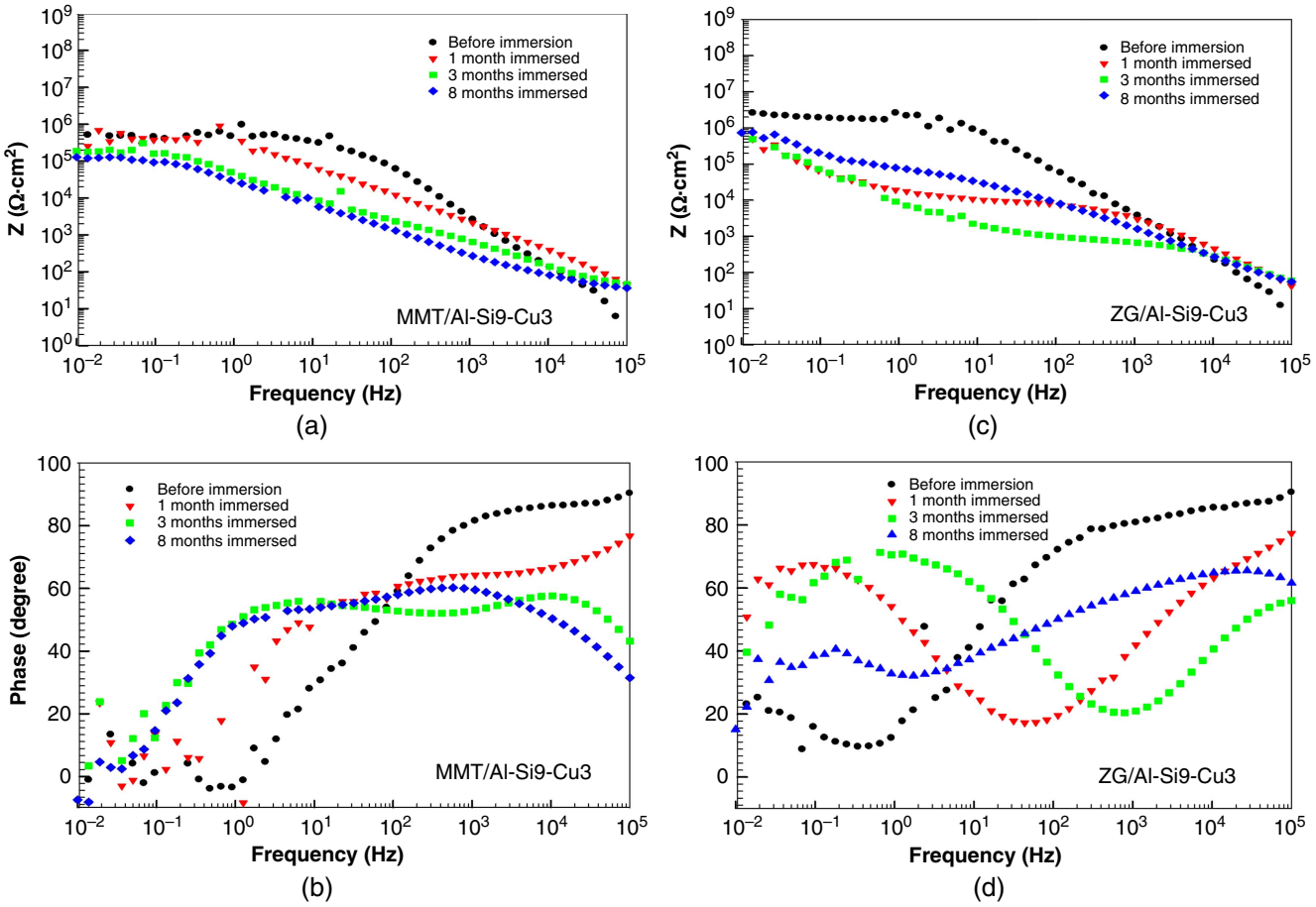

FIGURE 15. *Bode plots of (a, c) impedance magnitude and (b, d) phase angle as a function of frequency recorded in artificial seawater for Al-Si9-Cu3 samples coated with (a, b) MMT and (c, d) ZG before immersion in the Adriatic Sea and after 1, 3, and 8 months immersion. Before electrochemical measurements, the samples were sonicated to remove the biofilm formed during immersion in the seawater.*

that of MMT coating, reaching even higher |Z| values (Figures 15[c] and [d]).

After immersion in the Adriatic Sea, some coating deterioration can be noticed: E_{corr} shifted more positively, j_{corr} progressively increased, and the current density within the passive plateau (Figure 14[b], Table 5). The R_p values decreased to the initial state but were larger for two orders of magnitude. Therefore, compared to bare samples, MMT and ZG coatings still showed a considerable level of protection of Al-Si9-Cu3 even after 8 months of immersion, as corroborated by EIS results (Figures 15[c] and [d]).

3.6.2 | Al-Si7-Mg0.3 Coated Samples

The electrochemical response of Al-Si7-Mg0.3 coated samples indicates that both coatings assured the establishment of a broad passive region. For the MMT-coated sample, E_{br} was not observed in the measured range, whereas that of ZG-coated samples was ΔE 1,080 mV (Figure 16, Table 6). E_{corr} shifted to 200 mV more negative than the bare sample, j_{corr} was reduced by 3 orders of magnitude, and R_p was in the MΩ·cm^2 range. The EIS response confirmed the barrier character of the deposited coatings (Figures 17[a] and [b]).

After immersion, the measured current densities for the MMT-coated sample progressively increased and ΔE narrowed; however, compared to bare alloy, the protection was still high, as also reflected in large R_p values reaching 34 MΩ·cm^2 compared to 19 kΩ·cm^2 for the bare sample.

A similar situation was observed for the ZG-coated Al-Si7-Mg0.3 sample (Figures 16[b], 17[c], and [d]). The electrochemical parameters confirm the protective behavior of MMT and ZG coatings, especially on the Al-Si7-Mg0.3 substrate, which improved its protectiveness with immersion time (Part 1, Figure 19).

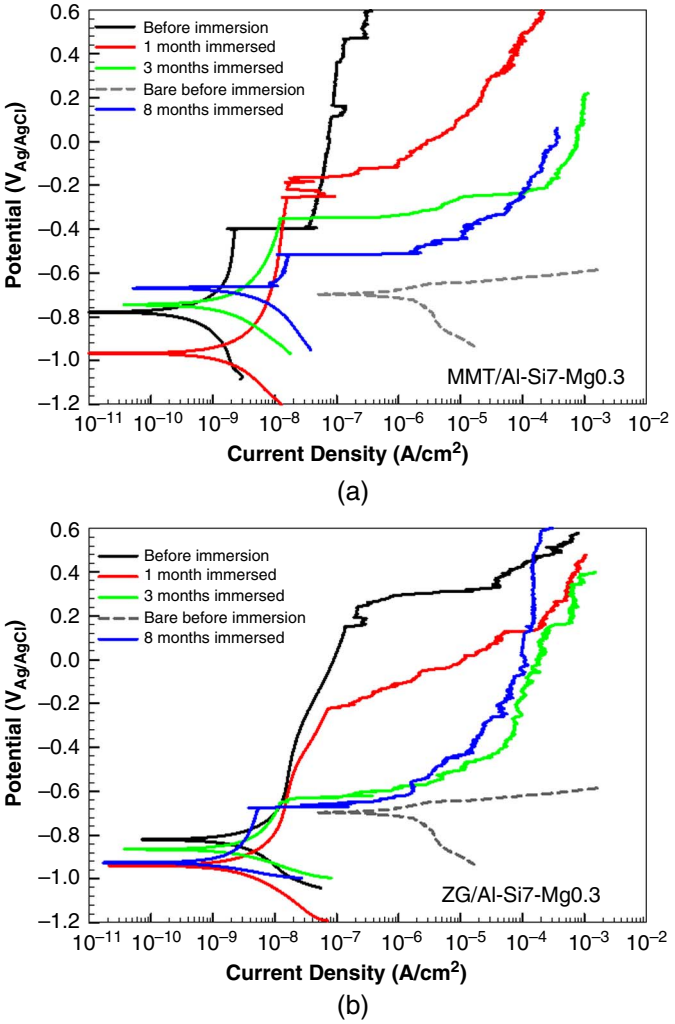

FIGURE 16. *Potentiodynamic polarization curves recorded in artificial seawater for Al-Si7-Mg0.3 coated with (a) MMT and (b) ZG coatings before immersion in the Adriatic Sea and after 1, 3, and 8 months of immersion. Before electrochemical measurements, the samples were sonicated to remove the biofilm formed during immersion in the seawater. The electrochemical parameters deduced from potentiodynamic curves are presented in Table 6. Curves for bare, nonimmersed samples are given for comparison.*

Table 6. *The Electrochemical Parameters Deduced from the Potentiodynamic Polarization Curves (Figure 16) Recorded for Al-Si7-Mg0.3 Samples Coated with MMT and ZG Coatings Before and After Immersion for 1, 3, and 8 Months in the Adriatic Sea*[(A)]

Condition	E_{corr} (V)	j_{corr} (μA/cm^2)	R_p (kΩ·cm^2)	E_{br} (V) (ΔE [mV])
Al-Si7-Mg0.3				
Before immersion	−0.69±0.01	1.06±0.03	16±1	−0.65 V (40 mV)
1 month immersed	−0.58±0.04	0.03±0.01	198±29	−0.005 V (575 mV)
3 months immersed	−0.67±0.05	0.07±0.02	411±143	0.09 V (760 mV)
8 months immersed	−0.66	2.57	19	−0.003 V (657 mV)
Al-Si7-Mg0.3/MMT				
Before immersion	−0.85±0.06	0.0009 ±0.0002	68467 ±1172	–
1 month immersed	−0.85±0.08	0.02±0.009	5299 ±2039	−0.17 V (680 mV)
3 months immersed	−0.82±0.07	0.0056 ±0.004	10744 ±8364	−0.35 V (470 mV)
8 months immersed	−0.67±0.04	0.004 ±0.003	34231 ±32109	−0.53 V (140 mV)
Al-Si7-Mg0.3/ZG				
Before immersion	−0.85±0.01	0.003 ±0.001	8344 ±2081	0.23 V (1,080 mV)
1 month immersed	−0.99±0.05	0.003 ±0.001	7943 ±1263	−0.23 V (760 mV)
3 months immersed	−0.89±0.10	0.003 ±0.001	7331 ±2070	−0.66 V (230 mV)
8 months immersed	−0.93±0.10	0.001 ±0.002	25668 ±992	−0.67 V (260 mV)

[(A)] The samples were sonicated before the analysis. The results for bare samples are given for comparison (already presented in Table 8 in Part 1).

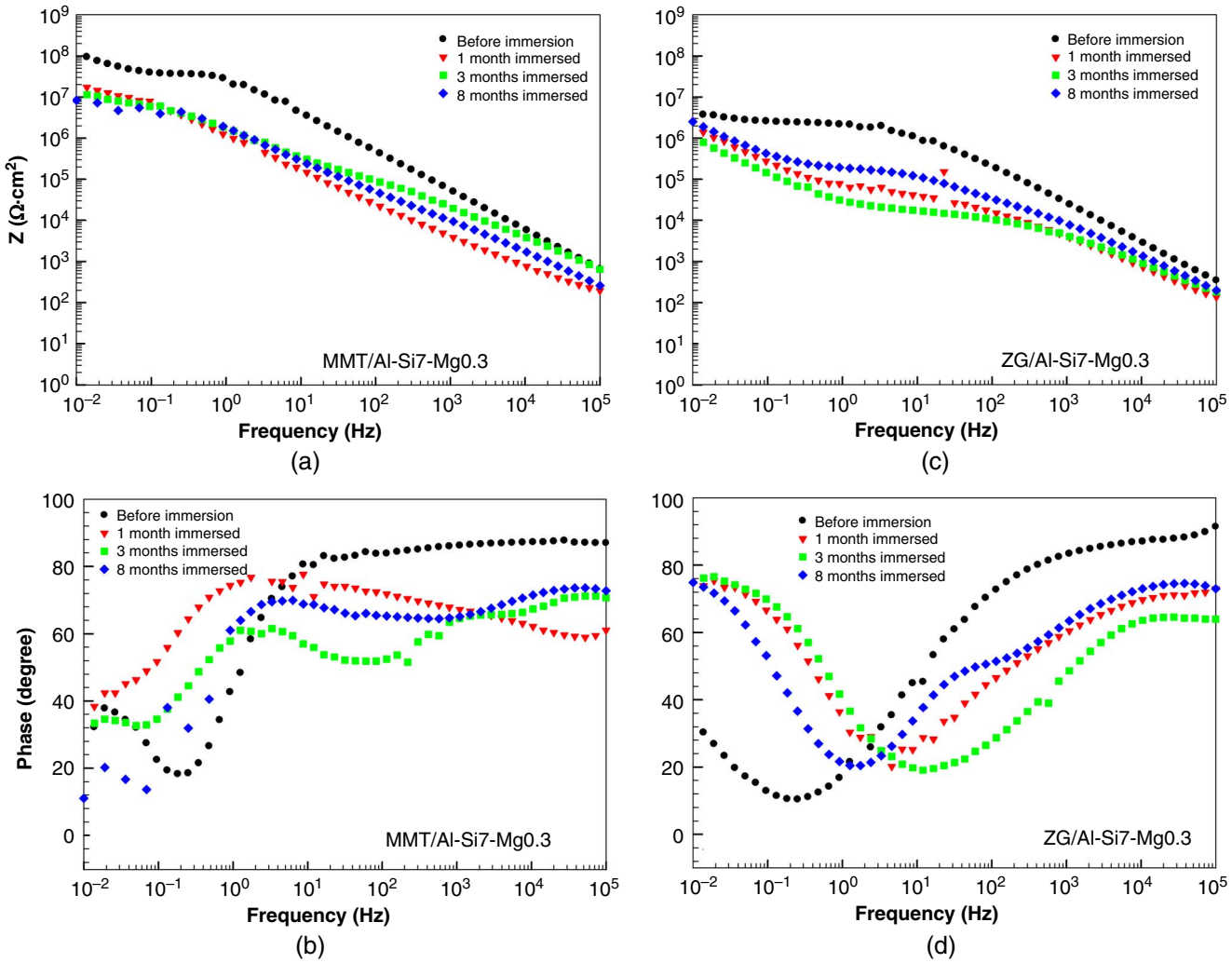

FIGURE 17. *Bode plots of (a, c) impedance magnitude and (b, d) phase angle as a function of frequency recorded in artificial seawater for Al-Si7-Mg0.3 samples coated with (a, b) MMT and (c, d) ZG before immersion in the Adriatic Sea and after 1, 3, and 8 months immersion. Before electrochemical measurements, the samples were sonicated to remove the biofilm formed during immersion in the seawater.*

CONCLUSIONS

Two cast aluminum alloys, Al-Si9-Cu3 and Al-Si7-Mg0.3, were coated with hybrid sol-gel coatings and characterized before and after immersion testing in the Adriatic Sea using SEM, XPS, and GDOES. Further, nonimmersed and immersed samples were investigated by electrochemical measurements in artificial seawater to follow the passivation and degradation processes on the coatings due to the immersion. The level of biofouling was documented after the designed immersion period. Sonication was used as a procedure to remove biofouling, simulating vessels in motion, or a simple mechanical cleaning step.

➢ Both coatings are hybrid, i.e., contain an inorganic part of the sol-gel network and an organic, polymerized part of the network. The coatings were prepared in two steps using two separately prepared solutions. MMT acrylate-based coating contains the inorganic part of Si–O–Si siloxane bonds intermixed with an organic polymerized acrylate network. ZG epoxy-based coating contains the inorganic part of Zr–O–Zr and Zr–O–Si bonds intermixed with the polymerized organic network. XPS analysis confirmed that the coatings are mainly organic and contain Si (IV) oxide (in MMT) and Si(IV) and Zr(IV) oxides (in ZG).

➢ The coatings decrease the surface's wettability, are homogeneous and dense, and have nanostructured morphology.

➢ After 8 months of immersion in the Adriatic Sea, a biofouling layer was formed, but it was removed in a significant proportion by sonication, especially for Al-Si7-Mg0.3 alloy. The coatings remained shiny and virtually intact. XPS analysis revealed that Al was detected at the coating surface after immersion, indicating some dissolution through the pores. However, the coatings' structure was preserved.

➢ Electrochemical measurements confirmed that both hybrid sol-gel coatings MMT and ZG deposited on cast Al-Si alloys acted as barriers, but better characteristics were obtained when deposited on Al-Si7-Mg0.3 alloy. Based on the results obtained, we can corroborate that these coatings are promising candidates for marine applications acting on the fouling-release principle.

ACKNOWLEDGMENTS

This work is a part of the M-ERA.NET project entitled "*Design of corrosion resistant coatings targeted for versatile applications*" (acronym COR_ID). The financial support of the project by MESS (Ministry of Education, Science, and Sport of the

Republic of Slovenia) and ANR (The French National Research Agency) is acknowledged. This work is also a part of the bilateral Proteus program between Slovenia and France entitled "DCOIN: Disentangling COrrosion and its INhibition," INCOR: INterfaces relevant for CORrosion and its inhibition," financed by the Slovenian Research Agency (SRA) and the ANR (Grant No. BI-FR/21-22-008). The financial support from the SRA (research core funding No. P2-0393 and No. P1-0134) is acknowledged. Partial funding of the XPS equipment by Région Ile-de-France is acknowledged. The authors acknowledge the Centre of Excellence in Nanoscience and Nanotechnology—Nanocenter (CENN), Ljubljana, Slovenia, to access the scientific equipment (FIB-SEM/EDS). The authors acknowledge D. Zimerl, G. Šekularac, D. Hamulić, and U. Tiringer for valuable help with sample preparation and Prof. A. Cör and Dr. K. Šuster for valuable discussions. The authors also thank co-workers of the Marine Biology Station of the National Institute of Biology in Piran, Slovenia: Dr. A. Ramšak for the expert discussion, Dr. V. Malačič for providing data from the Vida buoy, and diver T. Makovec for handling the samples. The company Talum d. d. Tovarna aluminija Kidričevo, Slovenija, is acknowledged for production and providing the cast Al-Si alloys.

References

1. I. Milošev, B. Kapun, P. Rodič, Ch. Carriérre, D. Mercier, S. Zanna, P. Marcus, *Corrosion* 79, 2 (2023): p. 193-212.
2. M.P. Schultz, J.A. Benedick, E.R. Holm, W.M. Hertel, *Biofouling* 27 (2011): p. 87-98.
3. A.G. Nurioglu, A.C.C. Esteves, G. de With, *J. Mater. Chem. B* 3 (2015): p. 6547-6570.
4. https://www.imo.org/en/OurWork/Environment/Pages/Anti-fouling.aspx.
5. R.G. Uc-Peraza, Í.B. Castro, G. Fillmann, *Sci. Total Environ.* 805 (2022): p. 150377.
6. J. Karlsson, E. Ytreberg, B. Eklund, *Environ. Pollut.* 158 (2010): p. 681-687.
7. T. Ren, G.-H. Fu, T.-F. Liu, K. Hu, H.-R. Li, W.-H. Fang, X.-L. Yang, *Fish Physiol. Biochem.* 43 (2017): p. 1-9.
8. S. Brendel, É. Fetter, C. Staude, L. Vierke, A. Biegel-Engler, *Environ. Sci. Eur.* 30 (2018): p. 9.
9. D. Meseguer Yebra, S. Kiil, K. Dam-Johansen, *Prog. Org. Coat.* 50 (2004): p. 75-104.
10. R. Ciriminna, F.V. Bright, M. Pagliaro, *ACS Sustain. Chem. Eng.* 3 (2015): p. 559-565.
11. M.R. Detty, R. Ciriminna, F.V. Bright, M. Pagliaro, *Acc. Chem. Res.* 47 (2014): p. 678-687.
12. J.E. Gittens, T.J. Smith, R. Suleiman, R. Akid, *Biotechnol. Adv.* 31 (2013): p. 1738-1753
13. J.A. Callow, M.E. Callow, *Nat. Commun.* 2 (2011): p. 244.
14. I. Banerjee, R.C. Pangule, R.S. Kane, *Adv. Mater.* 23 (2011): p. 690-718.
15. A.M.C. Maan, A.H. Hofman, W.M. de Vos, M. Kamperman, *Adv. Funct. Mater.* 30 (2020): p. 2000936.
16. P. Rodič, J. Iskra, I. Milošev, *J. Non-Cryst. Solids* 396-397 (2014): p. 25-35.
17. P. Rodič, J. Iskra, I. Milošev, *J. Sol-Gel Sci. Technol.* 70 (2014): p. 90-103.
18. P. Rodič, I. Milošev, *J. Electrochem. Soc.* 161 (2014): p. C412-C420.
19. P. Rodič, A. Mertelj, M. Borovšak, A. Benčan, D. Mihailović, B. Malič, I. Milošev, *Surf. Coat. Technol.* 286 (2016): p. 388-396.
20. P. Rodič, J. Katić, D. Korte, P.M. Desimone, M. Franko, S.M. Cére, M. Metikoš-Huković, I. Milošev, *Metals* 8 (2018): p. 248.
21. P. Rodič, I. Milošev, M. Lekka, F. Andreatta, L. Fedrizzi, *Prog. Org. Coat.* 124 (2018): p. 286-295.
22. P. Rodič, R. Cerc Korošec, B. Kapun, A. Mertelj, I. Milošev, *Polymers* 12 (2020): p. 948.
23. D. Hamulić, P. Rodič, M. Poberžnik, M. Jereb, J. Kovač, I. Milošev, *Coatings* 10 (2020): p. 172.
24. D. Hamulić, P. Rodič, I. Milošev, *Prog. Org. Coat.* 150 (2021): p. 105982.
25. P. Rodič, S. Zanna, I. Milošev, P. Marcus, *Front. Mater.* 8 (2021): p. 756447.
26. I. Milošev, D. Hamulić, P. Rodič, Ch Carrière, S. Zanna, H. Budasheva, D. Korte, M. Franko, D. Mercier, A. Seyeux, P. Marcus, *Appl. Surf. Sci.* 574 (2022): p. 151578.
27. I. Milošev, B. Kapun, P. Rodič, J. Iskra, *J. Sol-Gel Sci. Technol.* 74 (2015): p. 447-459.
28. R.B. Figueira, *Polymers* 12 (2020): p. 689.
29. R.B. Figueira, C.J.R. Silva, E.V. Pereira, *J. Coat. Technol. Res.* 12 (2015): p. 1-35.
30. D. Hamulić, I. Putna-Nimane, I. Liepina-Laimane, I. Dimante-Deimantovica, P. Rodič, I. Milošev, *J. Coat. Technol. Res.*, https://link.springer.com/article/10.1007/s11998-022-00701-2#article-info.